Acoust. Sci. & Tech. **31**, 1 (2010)

PAPER

Development of energy-based calculation methods of noise radiation from semi-underground road using a numerical analysis

Shinichi Sakamoto*

Institute of Industrial Science, The University of Tokyo

(*Received 7 April 2009, Accepted for publication 31 July 2009*)

Abstract: As a calculation method of road traffic noise at the roadside area of a semi-underground road, the "hypothetical point source method" was proposed in the road traffic noise prediction model "ASJ RTN-Model" proposed by the Acoustical Society of Japan. In this method, noise radiation from a straight semi-underground road is simply modeled as sound propagation from a hypothetical point source that has a directivity specific to the dimensions of the structure and is assumed to be at the center of the mouth. In the ASJ RTN-Model 2003, the directivity characteristics were determined on the basis of the results of a scale model experiment, and the variation of the applicable dimensions of the road structures was limited. In this paper, the directivity characteristics of the hypothetical point source are examined by wave-based numerical analysis to extend the variation. In the numerical analysis, a Fourier-type transformation technique from a two-dimensional field to a three-dimensional field is applied to the calculation results obtained by the two-dimensional finite-difference time-domain method. In addition, the practical expression of the sound power of the hypothetical sound source is investigated.

Keywords: Noise barriers, ASJ RTN-Model, Semi-underground road, Wave-based numerical analysis

PACS number: 43.50.Lj, 43.28.Js [doi:10.1250/ast.31.75]

1. INTRODUCTION

As a means of mitigating the propagation of road traffic noise, depressed or semi-underground roads are often constructed in Japan. In such cases, it is difficult to predict the noise propagation from the road structures to the roadside areas, because noise propagation inside the structure is very complicated owing to multiple reflections and diffraction.

As a practical noise prediction method for roadside areas of these road structures, energy-based calculation models are proposed in the ASJ RTN-Model published by the Acoustical Society of Japan. One of them is the image source method, in which multiple reflections between retaining walls of the structure and diffraction over the edges of the walls are considered. This method can be applied to depressed roads and semi-underground roads with relatively small overhangs, but it becomes difficult to apply this calculation model to the cases where the overhangs are large, because of a limitation in applying simple geometrical acoustics in such a complicated sound field. For such cases, another practical calculation method, in which noise radiation from the semi-underground road is modeled as sound propagation from a hypothetical directional point source, was also shown in the ASJ RTN-Model. The calculation method has been developed on the basis of a scale model experiment and the applicable road structures have been limited [1,2]. Upon the revision of the ASJ RTN-Model, the author investigated the practical calculation method based on a wave-based numerical analysis using the finite-difference time-domain (FDTD) method in order to extend the applicability of the method. In the wave-based numerical analysis, a Fourier-type transformation technique of a two-dimensional (2-D) response to a three-dimensional (3-D) response [3] was applied to the calculation results of transient responses obtained by the FDTD method. From the obtained 3-D responses, the values of several model parameters included in the practical calculation model of the "hypothetical point source method" were determined and the applicability of these parameters was examined. In this paper, the investigation based on the numerical analysis and the determinations of the values of the model parameters are described.

*e-mail: sakamo@iis.u-tokyo.ac.jp

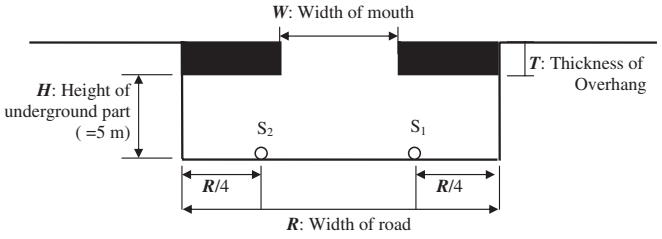

Fig. 1 Cross-sectional shape of semi-underground road under investigation.

Table 1 Variation of dimensions of the road structure.

	R	*T*	*W*
Case 1	20 m	1 m	5 m
Case 2			7.5 m
Case 3			10 m
Case 4			15 m
Case 5		4 m	5 m
Case 6			7.5 m
Case 7			10 m
Case 8			15 m
Case 9	30 m	1 m	5 m
Case 10			7.5 m
Case 11			10 m
Case 12			15 m
Case 13		4 m	5 m
Case 14			7.5 m
Case 15			10 m
Case 16			15 m

2. NUMERICAL ANALYSIS

2.1. Semi-Underground Road under Investigation

In this study, a straight semi-underground road with a symmetric cross section was considered, as shown in Fig. 1. The parameters characterizing this type of road structure are the width of the road, R, width of the mouth, W, height of the underground part of the road structure, H, and the thickness of the overhangs, T. The value of H was made constant ($= 5$ m) and sixteen combinations of the other three parameters were chosen, as shown in Table 1. All of the surfaces of the road structure were reflective. As sound sources, two incoherent sources with the same sound energy level of 100 dB were assumed to be at the center of each driving lane on the road surface. Therefore, the total sound energy level generated inside the road structure is 103 dB.

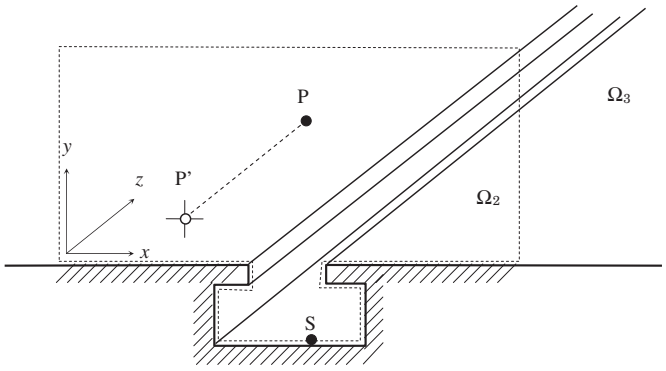

Fig. 2 Sound field with uniform cross section in z-direction, Ω_3 being the 3-D domain and Ω_2 being the 2-D domain.

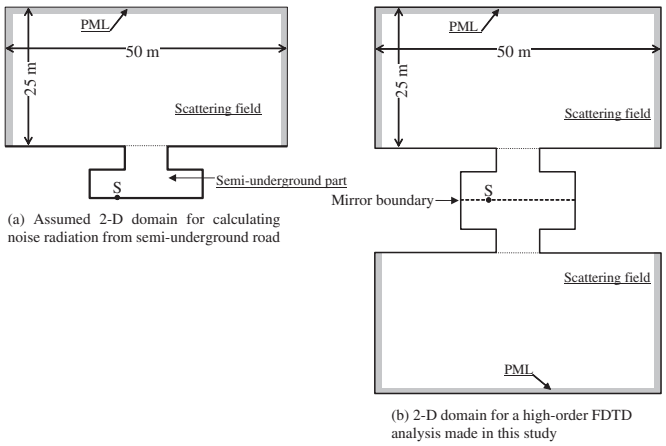

Fig. 3 Setting of domain for 2-D FDTD analysis.

2.2. FDTD Analysis

For a 3-D sound field with uniform geometry, a sound pressure response for a point source can be obtained from a 2-D solution using a Fourier-type integration [3]. This technique was applied to the calculation results obtained from 2-D numerical analysis of the cross-section of the semi-underground roads, as shown in Fig. 2. A 3-D response at point P is calculated from the 2-D solution at point P′ obtained by 2-D FDTD analysis. Figure 3(a) shows the 2-D sound field for the 2-D FDTD analysis. The sound field inside the semi-underground road and a scattering field with a width of 50 m and height of 25 m were modeled for the analysis. Around the scattering field, perfectly matched layers (PML) [4,5] were set in order to realize nonreflecting termination. As FDTD calculation conditions, the discrete spatial grid size and time step interval were 0.025 m and 0.01 ms, respectively. In the sound field inside the semi-underground structure with rigid surfaces, multiple reflections and diffraction occur and the duration of the transient response becomes long. Therefore, the number of calculation steps was 600,000 (6 seconds). As a sound source condition, the initial sound pressure distribution with the following Gaussian profile was adopted:

$$p_0(r) = \exp\left(-\frac{r^2}{d^2}\right), \tag{1}$$

where $r = \sqrt{(x-x_s)^2 + (y-y_s)^2}$, in which (x_s, y_s) is the coordinate of a source point, and d is a constant and equal to 0.05 m in this study. To reduce dispersion error, a fourth-order spatial finite difference scheme was adopted [6]. In reality, the calculation accuracy of the high-order scheme used in this calculation decreased when a source was located at a boundary. Therefore, this analysis was conducted for the sound field shown in Fig. 3(b). Sound propagation in the upper or lower half-space in Fig. 3(b) is theoretically identical with that in Fig. 3(a) according to the principle of mirror image.

In order to examine directivity characteristics of sound radiation from the mouth of the semi-underground road, 102 receiving points were distributed on the quarter-spherical surface of 20 m radius, as shown in Fig. 4. Hereafter in this study, the positions of receiving points are indicated in polar coordinates as $(\bar{r}, \theta, \varphi)$, where $\bar{r}$ is a constant of 20 m.

2.3. Analysis of Calculation Results

From the calculation results of the 2-D FDTD analysis, 3-D impulse responses at all receiving points were obtained by the 2-D to 3-D transformation [3]. The detailed procedure of the transformation is described in [3]. In the transformation from 2-D to 3-D, the fast Fourier transform (FFT) algorithm was used in order to obtain frequency components from transient responses calculated by the 2-D FDTD, and the number of FFT points set in the transformation was 524,288 (2^{19}), and consequently, the frequency resolution for the integration became 0.19 Hz. An example of the responses is shown in Fig. 5. On the basis of such 3-D impulse responses, directivities of sound radiation are examined. In the energy-based practical calculation model proposed in the ASJ RTN-Model, the A-weighted sound pressure level is directly calculated. Therefore, in this study, the A-weighted single event sound exposure level was calculated from the 3-D impulse response, under the condition that the A-weighted sound energy level of a sound source was 100 dB. The procedure for obtaining the A-weighted single event sound exposure level is as follows.

[1] Calculation of single event sound exposure level at receiving point

Frequency components of the 3-D impulse response at a receiving point positioned at $(\bar{r}, \theta_i, \varphi_i)$ are calculated by FFT, and a band level in each 1/3 octave band, $L_{E,S}(f_{c,k}, \theta_i, \varphi_i)$, is obtained by integrating squared values of frequency components included in the objective band. Here, θ_i and φ_i mean azimuth and elevation angles of the i-th receiving point, respectively, and $f_{c,k}$ means the center frequency of the k-th band. The calculated values are band levels under the sound source condition of a certain Gaussian pulse expressed by Eq. (1), and the source has

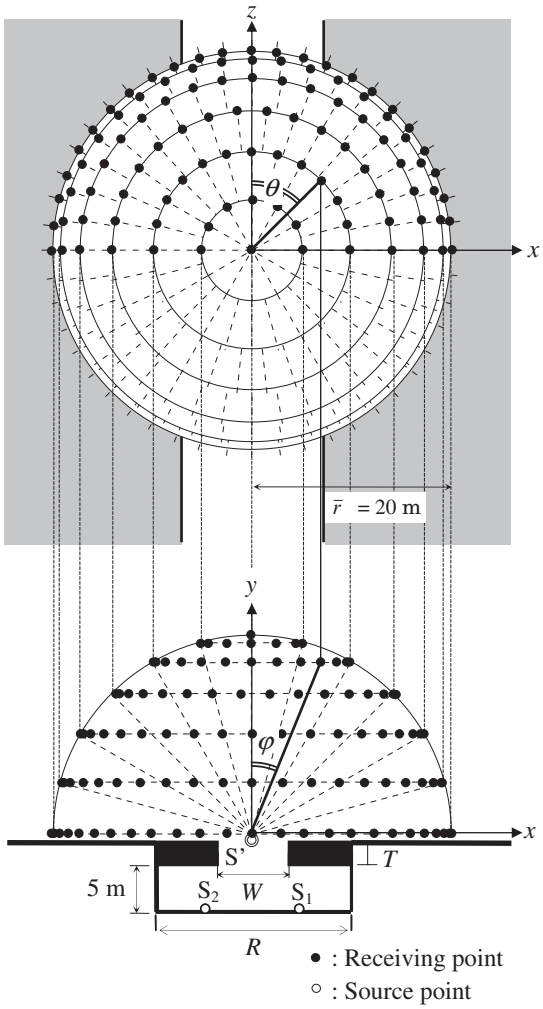

Fig. 4 Geometrical setting of semi-underground road, sound sources and receiving points in the calculation.

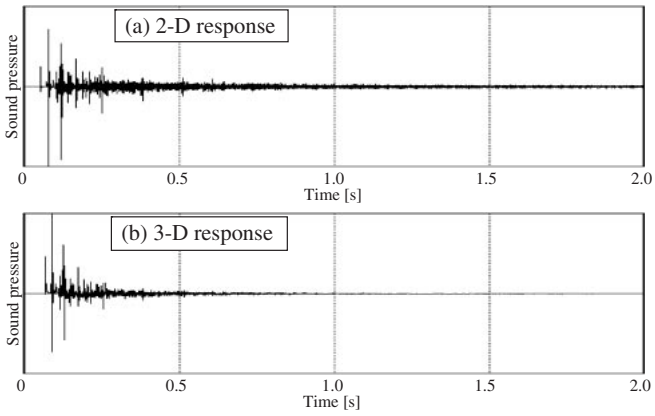

Fig. 5 Example of impulse response (a) calculated for 2-D domain by the FDTD method and (b) transformed from 2-D response to 3-D response, at a receiving point $(\bar{r}, 60^\circ, 60^\circ)$ for Case 2.

spectral characteristics specific to the source condition. Therefore, at first, the frequency characteristics of the sound energy of the source should be evaluated in order to appropriately correct the calculation results at receiving points.

[2] Sound energy level of source

The sound energy level of the source was determined from 3-D responses calculated under the free field condition. To accomplish this determination, an additional 2-D FDTD analysis for a free field and transformation processing from 2-D to 3-D were conducted. In the 2-D FDTD analysis, the discrete spatial grid size, the time interval and the initial condition were the same as those of 2-D FDTD for the sound field in which a semi-underground road existed. From the calculation results of the 3-D impulse response, the single event sound exposure level in each 1/3 octave band was obtained through FFT, and the sound energy level of the source was calculated considering the distance between the source and the receiving point.

[3] Correction of spectral characteristics

In ASJ RTN-Model 2008, the correction terms of the spectral characteristics of running vehicle noise, $\Delta L_{\mathrm{RTN}}(f_{\mathrm{c},k})$, are specified as a function of frequency, as

$$\Delta L_{\mathrm{RTN}}(f_{\mathrm{c},k}) = -20\log_{10}\left[1+\left(\frac{f_{\mathrm{c},k}}{2500}\right)^2\right]. \qquad (2)$$

Considering the spectral characteristics of the sound energy level of a source set in the numerical analysis, of running vehicle noise, and of A-weighting denoted by $\Delta L_{\mathrm{A}}(f_{\mathrm{c},k})$, the values of correction regarding spectral characteristics, $\Delta L_{\mathrm{c}}(f_{\mathrm{c},k})$, is calculated as

$$\begin{aligned}\Delta L_c(f_{\mathrm{c},k}) = &-L_J(f_{\mathrm{c},k}) + \Delta L_{\mathrm{RTN}}(f_{\mathrm{c},k}) \\ &+ \Delta L_{\mathrm{A}}(f_{\mathrm{c},k}) + \Delta L_{\mathrm{adj}}(f_{\mathrm{c},k}),\end{aligned} \qquad (3)$$

where $L_J(f_{\mathrm{c},k})$ is the sound energy level in the k-th frequency band of the source set in the FDTD analysis, $\Delta L_{\mathrm{adj}}(f_{\mathrm{c},k})$ is an adjusting term to render the overall sound energy level of the source 100 dB.

The 1/3 octave band level, $L_{E,S}(f_{\mathrm{c},k}, \theta_i, \varphi_i)$, calculated from the 3-D impulse response at the i-th receiving point, is corrected with the correction term of $\Delta L_{\mathrm{c}}(f_{\mathrm{c},k})$ to obtain band levels of sound radiated from the sound source with an overall energy level of 100 dB, as follows:

$$L_E(f_{\mathrm{c},k}, \theta_i, \varphi_i) = L_{E,S}(f_{\mathrm{c},k}, \theta_i, \varphi_i) + \Delta L_c(f_{\mathrm{c},k}). \qquad (4)$$

[4] Calculation of A-weighted single event sound exposure level

The A-weighted single event sound exposure level at the i-th receiving point is calculated as the energy sum of the 1/3 octave band levels, as

$$L_{AE}(\theta_i, \varphi_i) = 10\log_{10}\left\{\sum_{k=1}^{N} 10^{L_E(f_{\mathrm{c},k}, \theta_i, \varphi_i)/10}\right\}, \qquad (5)$$

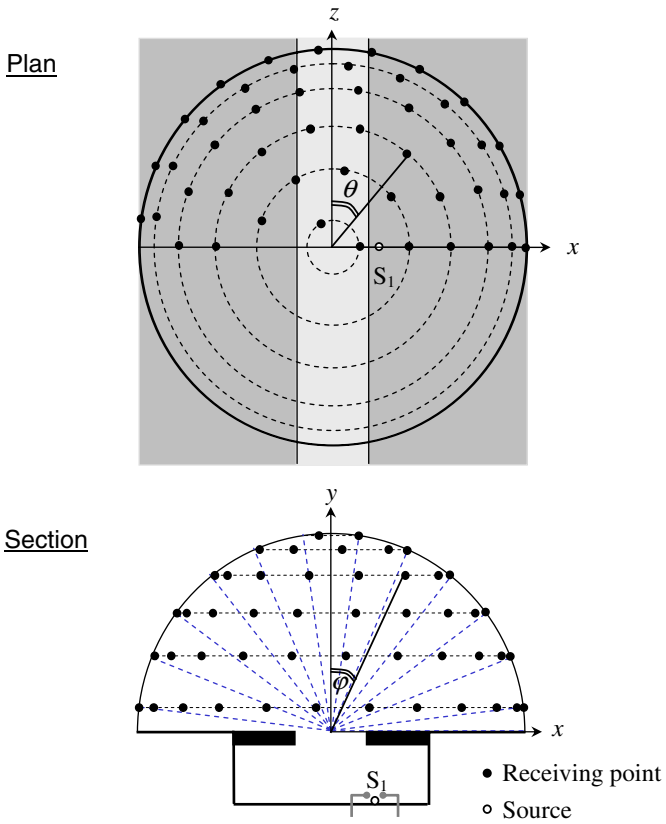

Fig. 6 Experimental setting of source and receiving points.

where N is the number of bands. From the A-weighted single event sound exposure levels calculated when the sound source was located at the source position of S_1, the single event sound exposure level at a point on an spherical surface at each azimuth angle θ ($\theta = -90°, -89°, \ldots, 89°, 90°$) and elevation angle φ ($\varphi = 0°, 1°, \ldots, 89°, 90°$) was calculated by spline interpolation in order to obtain detailed directivity characteristics of sound radiated from the mouth of the semi-underground road. The level for the case with the sound source at position S_2 was determined by considering the axis symmetry of the sound field. By summing these levels on an energy-base, the A-weighted single event sound exposure level was obtained for the case where two sound sources with the same sound energy level exist in the two driving lanes.

2.4. Comparison with Experimental Result

The calculated sound radiation characteristics were compared with the experimental results obtained with a scale model in order to validate the applicability of the calculation. A 1/20 scale model experiment of the sound radiation characteristics was carried out using a spark discharge impulse source [2]. Figure 6 shows the geometrical configuration of the sound source and the measurement points in the scale model experiment. As the sound source, a spark discharge impulse source was used to realize an omni directional point source, and it was

set at the position of S_1. To examine the directivity of the sound radiation from the mouth, a quarter-spherical measurement surface of 1 m (20 m in real scale) radius was set at the mouth so that its center was positioned on the centerline at the mouth in the source section. The measurement surface was divided into 44 subareas of almost equal area, and a measurement point was set on each of the subareas. In the experiment, impulse responses from a source to receiving points were measured, and the A-weighted single event sound exposure levels, assuming that the source had the spectral characteristics of running vehicle noise, were determined by the same procedure as for the calculation. The single event sound exposure levels at points on the measurement spherical surface at each azimuth angle θ ($\theta = -90°, -89°, \ldots, 89°, 90°$) and elevation angle φ ($\varphi = 0°, 1°, \ldots, 89°, 90°$) for the cases of a single source (S_1) and double sources (S_1 and S_2) were calculated by spline interpolation in the same manner as the calculation.

Figures 7(a) to 7(d) show the results of calculation and experiment for Cases 1, 2, 3 and 4 when a source was located at S_1, and Figs. 8(a) to 8(d) show the results for two sources located at S_1 and S_2. In these figures, the single event sound exposure levels on a receiving surface when the sources had a 100 dB sound energy level are shown in the form of a net graph. We can see that the radiation directivity varies with the sectional shape. In all cases, the directivity in the *x*-*y* plane is sharp in the upper and oblique directions, whereas that in the longitudinal section of the *y*-*z* plane is rather gentle. The agreement between the calculation results and the experimental results is fairly good. In order to elucidate the quantitative correspondence between the calculation and the experiment, as the most fundamental quantity, the total sound energy radiating from the mouth of the semi-underground structure was compared. In both of the calculation and the experiment, single event sound exposure levels at receiving points distributed on a hemispherical surface of $\bar{r} = 20$ m radius were obtained. Therefore, levels of total sound energy radiating from the mouth, $L_{JA,FDTD}$ from the calculation and $L_{JA,experiment}$ from the experiment, can be approximated by surface integration of sound exposures as

$$L_{JA,FDTD} = 10\log_{10}\left[\sum_{\theta,\varphi}\{10^{L_{AE,FDTD}(\theta,\varphi)/10}\cdot\Delta S(\theta,\varphi)\}\right], \quad (6)$$

$$L_{JA,experiment} = 10\log_{10}\left[\sum_{\theta,\varphi}\{10^{L_{AE,experiment}(\theta,\varphi)/10}\cdot\Delta S(\theta,\varphi)\}\right], \quad (7)$$

where $L_{AE,FDTD}(\theta,\varphi)$ and $L_{AE,experiment}(\theta,\varphi)$ are single event sound exposure levels at point $(\bar{r},\theta,\varphi)$ obtained by calculation and experimentally, respectively, and $\Delta S(\theta,\varphi)$ is the area of a segment of a spherical surface for point $(\bar{r},\theta,\varphi)$ (see Fig. 9). The result of the comparison is shown in Fig. 10. Differences between the calculation and experiment were within 1.4 dB for cases 1, 2, 3 and 4.

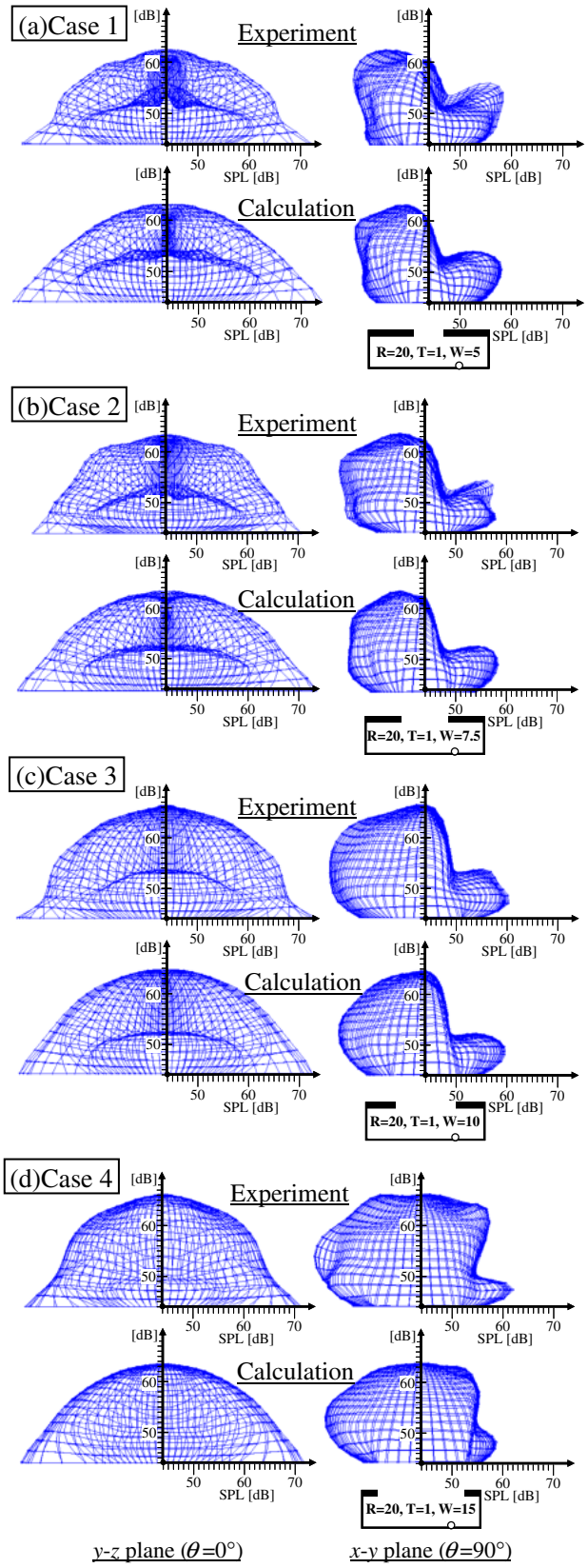

Fig. 7 Results of calculation and scale model experiment for the case where sound source is positioned at S_1.

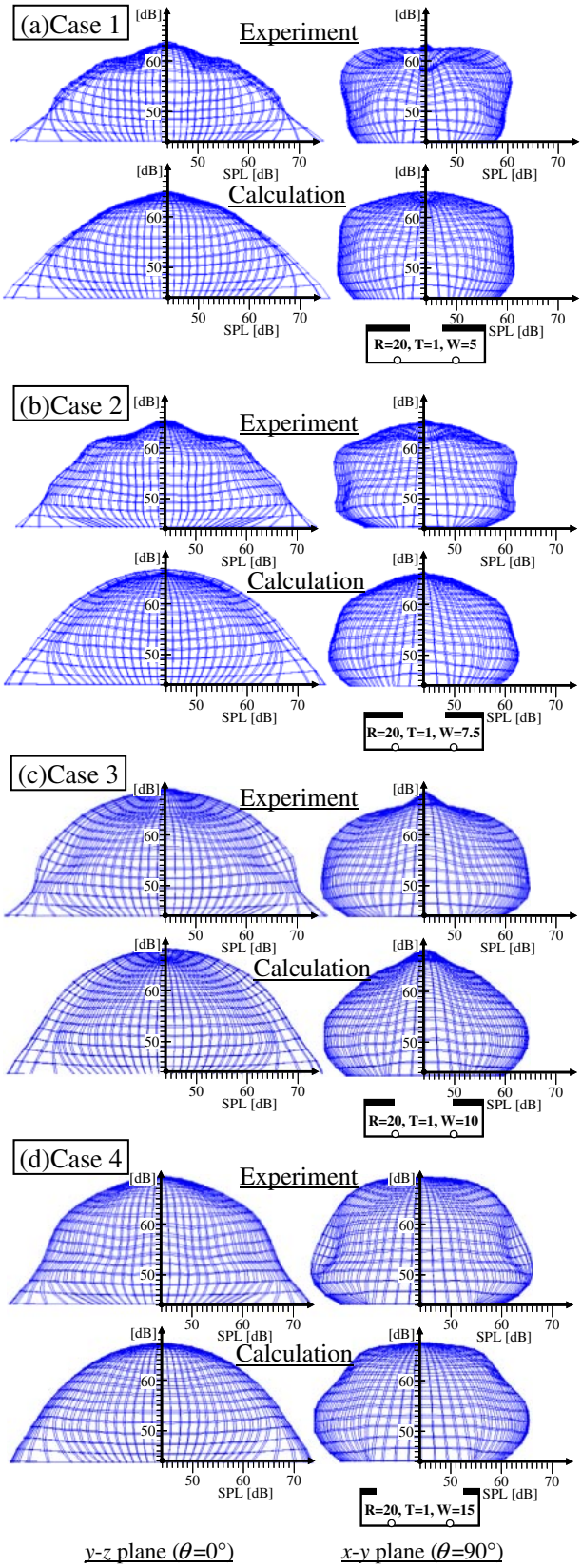

Fig. 8 Results of calculation and scale model experiment for the case where two sound sources are positioned at S_1 and S_2.

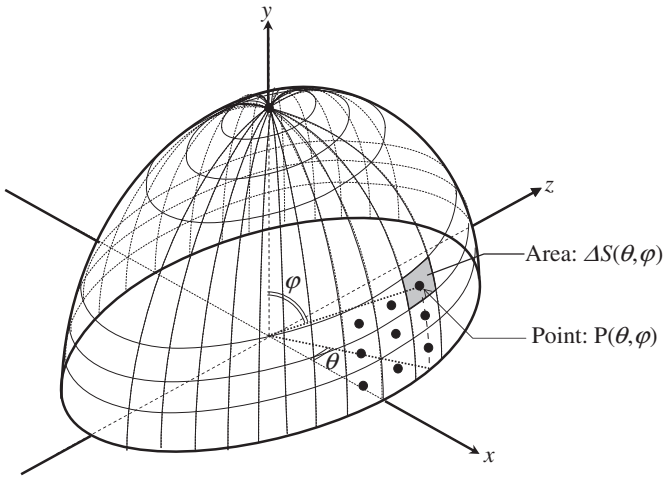

Fig. 9 Definition of area, ΔS, and receiving point, P.

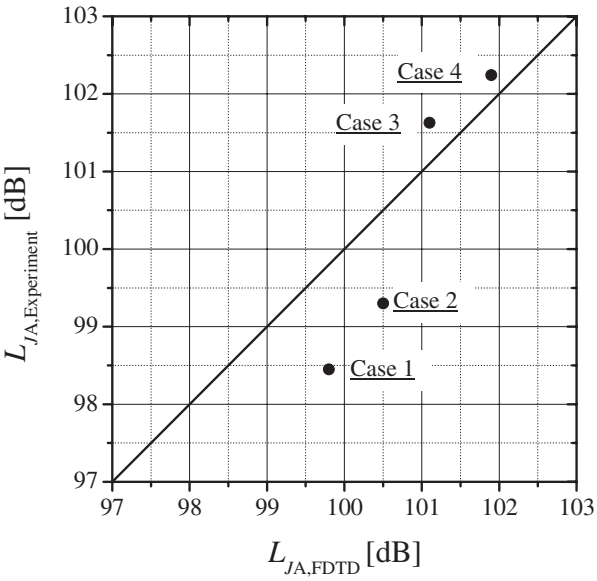

Fig. 10 Sound energy radiating from the mouth obtained by calculation and experiment.

3. DETERMINATION OF PARAMETERS IN ASJ RTN-Model

Sound radiation characteristics obtained by the numerical analysis described above are applied to the determination of model parameters in an energy-based practical calculation method, the "hypothetical point source method," included in ASJ RTN-Model 2008. Firstly, here, the hypothetical point source method is described briefly. It should be noted that the expressions for a stationary sound source of running road vehicles are described in the ASJ RTN-Model, whereas the transient sound source of a unit impulse is dealt with in this study. In this section, the descriptions in the ASJ RTN-Model are translated into those for transient sound source to gain physical corre-

spondence with the calculation results in this study. The relationship between the sound energy level, L_J, for a transient sound source and the single event sound exposure level, L_E, is equivalent to that between the sound power level, L_W, for a stationary sound source and the sound pressure level, L_p.

3.1. Hypothetical Point Source Method Specified in ASJ RTN-Model

Suppose a straight semi-underground road, which has asymmetrical cross section and equal traffic volume on both driving lanes, and a receiving point, P, as shown in Fig. 11. When sound sources are positioned at S_1 and S_2 with the total sound energy level of L_{JA}, the A-weighted single event sound exposure level at P, L_{AE}, is calculated using the following equations, as sound propagation from a hypothetical directional sound source, S′, located at a center point at the mouth of the semi-underground road structure.

$$L_{AE} = L_{JA,su} + 10\log_{10}\{a + (1-a)\cos^{n(\theta)}\varphi\} - 8 - 20\log_{10} r \quad (8)$$

$$n(\theta) = n_{max}\sin^{\beta}\theta \quad (9)$$

Here, $L_{JA,su}$ is the apparent sound energy level of a hypothetical sound source of S′, r is the distance from S′ to P, and a, n_{max} and β are model parameters that represent the directivity of sound radiation from the mouth. These parameters have specific values for the dimensions of the cross-sectional shape of the road structure. $L_{JA,su}$ is calculated as

$$L_{JA,su} = L_{JA} + \Delta L_{dim,su} + \Delta L_{dir,su} + \Delta L_{abs,su}, \quad (10)$$

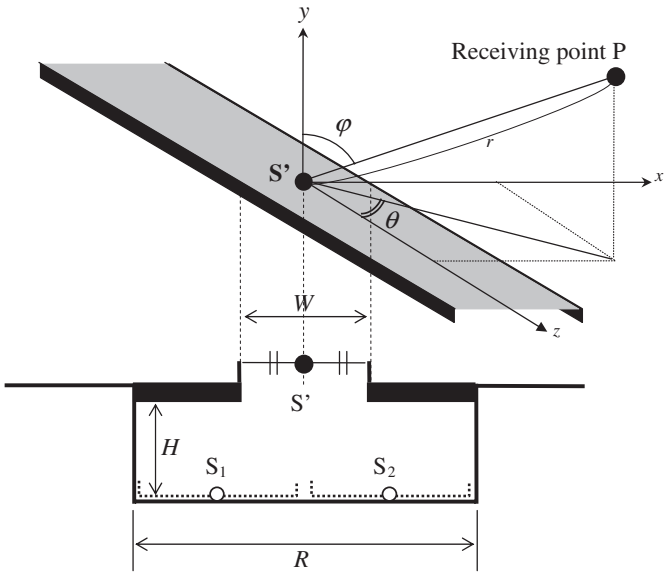

Fig. 11 Coordinate system for calculation of the hypothetical point source method.

where $\Delta L_{dim,su}$, $\Delta L_{dir,su}$ and $\Delta L_{abs,su}$ are correction terms for the dimensions of the road structure, the directivity of sound radiation and the absorbing condition inside the structure, respectively. The term $\Delta L_{dim,su}$ is dependent on the dimensions of the road structure R, W and H, and the determination of its value is described in the next section. The term $\Delta L_{dir,su}$ is a correction so as not to change the total amount of radiating sound energy when using a directivity function, and it is dependent on the model parameters of a, n_{max} and β, which characterize the directivity of sound radiation. The values of $\Delta L_{dir,su}$ are calculated using

$$\Delta L_{dir,su} = -10\log_{10}\left[\frac{\int_0^{2\pi}\int_0^{\pi/2}\{a + (1-a)\cos^{n_{max}\sin^{\beta}\theta}\varphi\}\sin\varphi d\varphi d\theta}{2\pi}\right]. \quad (11)$$

In this study, $\Delta L_{abs,su} = 0$ because semi-underground roads with reflective surfaces are dealt with.

Figure 12 shows examples of the polar pattern of noise radiation calculated by (a) numerical analysis and (b) the "hypothetical point source method" specified in Eqs. (8), (9) and (10). The practical calculation model simplifies the directivity of sound radiation, as shown in Fig. 12(b). The directivity is gentle in a y-z plane ($\theta = 0^\circ$), where the calculation model shows omnidirectional characteristics when the value of the directivity function of $n(\theta)$ is zero, as indicated in Eq. (9), whereas it is sharp in the x-y plane ($\theta = 90^\circ$).

3.2. Sound Energy Level of Hypothetical Sound Source

In the simplified calculation model described above, the sound energy level of the hypothetical source of S′ is assumed to be the total sound energy emitted through the mouth of the semi-underground road. In order to establish the calculation model of the sound energy level of S′, the total sound energy emitted through the mouth is discussed from the viewpoint of geometrical acoustics. Now, let us assume the following simplifications for a sound source existing inside the road structure and for sound propagation inside the semi-underground structure.

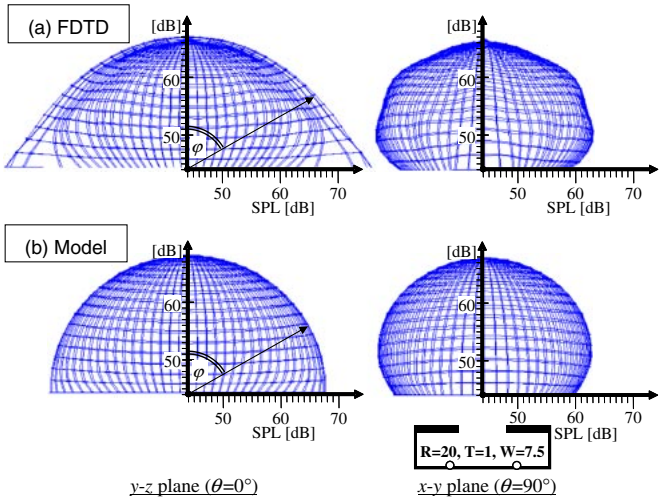

Fig. 12 Sound radiation characteristics obtained by (a) FDTD analysis and (b) ASJ RTN-Model, for Case 2.

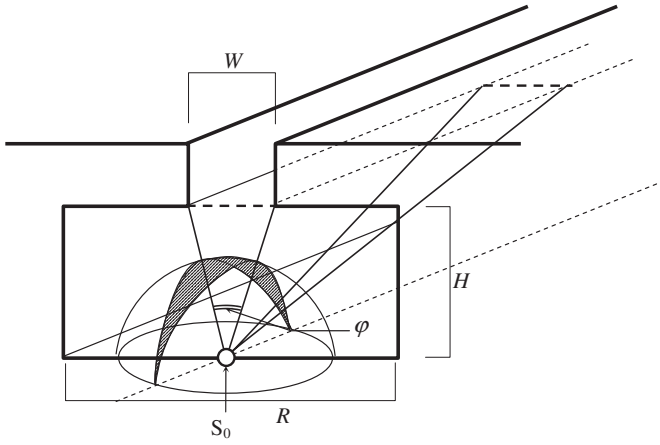

Fig. 13 Contribution of directly arriving sound energy.

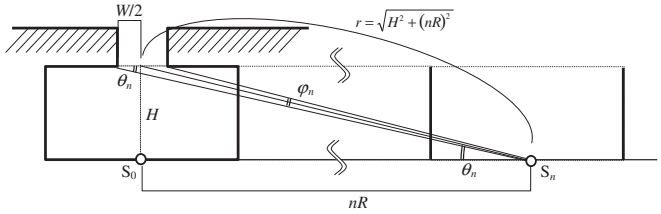

Fig. 14 Contribution of sound reflecting from a sidewall.

Assumption-1: Sound sources existing inside the structure (that is, the source on each driving lane) are lumped together as an omnidirectional point source positioned at the center of the road.

Assumption-2: Sound energy arriving at the mouth without reflecting from ceilings, and the road surface contributes sound radiation to the outside area; any multiple reflection path including reflection from the ceiling or from the road surface is ignored. That is, only sound reflection paths from sidewalls are considered.

Then, sound energy directly arriving at the mouth, E_0, is expressed below, for the case when a source with sound energy Q (sound energy level is made to be L_{JA}) exists in the semi-underground structure with road width R, semi-underground height of H and mouth width of W, as shown in Fig. 13.

$$E_0 = Q\frac{\varphi}{\pi} = Q\frac{2}{\pi}\tan^{-1}\frac{W}{2H}. \tag{12}$$

The components of reflected sound can be considered as the sound energy from a series of mirror image sources of sidewalls. Figure 14 illustrates the contribution from the n-th order image source. The contribution from the n-th order image source, E_n, is expressed as

$$E_n = Q\frac{\varphi_n}{\pi} \quad (n \geq 1). \tag{13}$$

When $nR \gg H$, the following relationships hold to a fair approximation.

$$\frac{W}{2}\sin\theta_n \approx \sqrt{H^2 + (nR)^2}\,\frac{\varphi_n}{2}, \tag{14}$$

$$\sin\theta_n \approx \frac{H}{\sqrt{H^2 + (nR)^2}}. \tag{15}$$

On the basis of the above relationships, φ_n can be expressed as

$$\varphi_n = \frac{WH}{(nR)^2}\left\{1 + \left(\frac{H}{nR}\right)^2\right\}^{-1} \approx \frac{WH}{R^2}\frac{1}{n^2} - \frac{WH^3}{R^4}\frac{1}{n^4}, \tag{16}$$

and consequently, sound energy from the n-th mirror image source can be approximated as

$$E_n \approx Q\left(\frac{WH}{\pi R^2}\frac{1}{n^2} - \frac{WH^3}{\pi R^4}\frac{1}{n^4}\right). \tag{17}$$

The total sound energy radiating from the mouth is given as the sum of directly arriving energy and contributions from a series of mirror images, as

$$E = E_0 + 2\sum_{n=1}^{\infty} E_n$$

$$= Q\left\{\frac{2}{\pi}\tan^{-1}\frac{W}{2H} + \frac{2WH}{\pi R^2}\sum_{n=1}^{\infty}\frac{1}{n^2} - \frac{2WH^3}{\pi R^4}\sum_{n=1}^{\infty}\frac{1}{n^4}\right\}. \tag{18}$$

Considering that infinite sums of series that appear in Eq. (18) are $\sum_{n=1}^{\infty} 1/n^2 = \pi^2/6$ and $\sum_{n=1}^{\infty} 1/n^4 = \pi^4/90$, the total sound energy and its level expression are approximately described by

$$E = Q\left(\frac{2}{\pi}\tan^{-1}\frac{W}{2H} + \frac{\pi WH}{3R^2} - \frac{\pi^3 WH^3}{45R^4}\right), \tag{19}$$

$$L_{JA,Model} = L_{JA}$$

$$+ 10\log_{10}\left(\frac{2}{\pi}\tan^{-1}\frac{W}{2H} + \frac{\pi WH}{3R^2} - \frac{\pi^3 WH^3}{45R^4}\right). \quad (20)$$

Consequently, the correction term regarding the dimensions of the road structure, $\Delta L_{\mathrm{dim,su}}$, in Eq. (10) is expressed as

$$\Delta L_{\mathrm{dim,su}} = 10\log_{10}\left(\frac{2}{\pi}\tan^{-1}\frac{W}{2H} + \frac{\pi WH}{3R^2} - \frac{\pi^3 WH^3}{45R^4}\right). \quad (21)$$

In order to confirm the validity of this approximation, the estimated sound energy calculated using Eq. (20) for all cases was compared with the calculation results obtained by the FDTD method. For the calculation of Eq. (20), L_{JA} was made to be 103 dB. To accommodate this situation, calculation results by the FDTD method, under the condition that the two sources S_1 and S_2 existed, were used and surface integration of the sound exposures on the receiving surface was accomplished in the same manner as described in 2.4 to estimate the total sound energy radiating from the mouth. Results of the comparison are shown in Fig. 15. The total energy radiating to the outside area tends to become lower as the width of the mouth becomes smaller. The difference between the two values is within 1.3 dB.

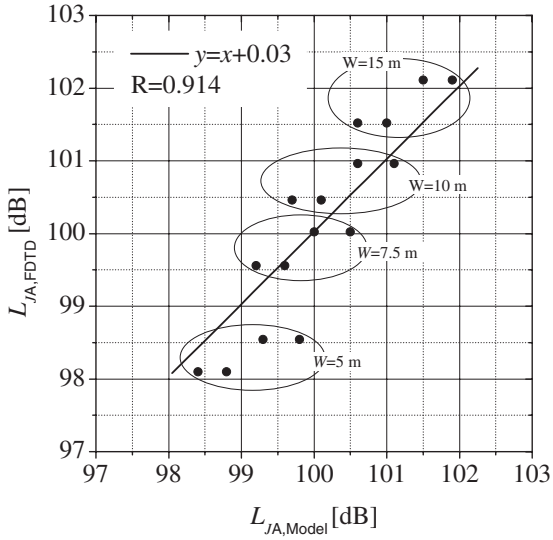

Fig. 15 Correspondence between total energy radiating from the mouth obtained by FDTD analysis and that obtained using Eq. (18).

3.3. Parameters Characterizing Directivity

Figure 8 indicates that the directivity of sound radiation characteristics varies with the cross-sectional shape of the road structure. Therefore, model parameters of a, $n_{\max}$ and β in Eqs. (8) and (9), which characterize the directivity of sound radiation are determined for all cases investigated in this study.

3.3.1. Determination procedure

In the practical calculation model expressed by Eqs. (8) and (9), a hypothetical sound source S′ can be regarded to have an omnidirectional component characterized by the parameter a, and a directional component. Here, let us express an omnidirectional and a directional component as $L_{\mathrm{AE,omni}}$ and $L_{AE,\mathrm{directional}}$, respectively; then the level of total sound exposure is expressed as the sum of the omnidirectional and directional components as follows:

$$L_{AE} = 10\log_{10}\{10^{L_{\mathrm{AE,omni}}/10} + 10^{L_{AE,\mathrm{directional}}/10}\}. \quad (22)$$

The minimum value of the directional components of $10^{L_{AE,\mathrm{directional}}/10}$ is zero because the directivity is modeled as the $n(\theta)$ power of a cosine function, as expressed in Eq. (8), and therefore, the omnidirectional components can be determined from the minimum sound exposure obtained on equidistant receiving points. Hence, firstly, the minimum single event sound exposure level, $L_{AE,\mathrm{Minimum}}$, of directivity characteristics obtained by the numerical analysis on a quarter spherical surface with 20 m radius was determined, and the sound energy level of the omnidirectional component, $L_{JA,O}$, was calculated as

$$L_{JA,O} = L_{AE,\mathrm{Minimum}} + 34. \quad (23)$$

To obtain the directional components, $L_{AE,\mathrm{directional}}(\theta,\varphi)$, included in the single event sound exposure levels at the observation surface, the value of $L_{AE,\mathrm{Minimum}}$ was subtracted from all single event sound exposure levels in energy-based as

$$L_{AE,\mathrm{directional}}(\theta,\varphi) = 10\log_{10}\{10^{L_{AE}(\theta,\varphi)/10} - 10^{L_{AE,\mathrm{Minimum}}/10}\}. \quad (24)$$

On the basis of the above values that represent directional components, parameters $n_{\max}$ and β are calculated by the method of least mean squares, which comprised the following two steps. First, for every azimuth angle of θ, a functional parameter of $n(\theta)$ is determined. When an omnidirectional component is subtracted from Eq. (8), the level of a directional component included in single event sound exposure at an observation point of $(\bar{r},\theta,\varphi)$ is expressed as

$$L_{AE,\mathrm{directional}} = L_{JA,\mathrm{directional}} + 10n(\theta)\log_{10}\{\cos\varphi\} - 34, \quad (25)$$

where $L_{JA,\mathrm{directional}} = L_{JA,su} + 10\log_{10}(1-a)$.

Now, assuming that $L_{JA,\mathrm{directional}}$ and $n(\theta)$ are unknown parameters in Eq. (25), the two values can be determined by the method of least mean squares based on $L_{AE,\mathrm{directional}}(\theta,\varphi)$ for every θ.

In the next step, $n_{\max}$ and β are calculated from the obtained values of $n(\theta)$. The logarithmic expression of Eq. (9) is

$$\log_{10} n(\theta) = \log_{10} n_{\max} + \beta \cdot \log_{10} \sin\theta. \quad (26)$$

Assuming that $\log_{10} n_{\max}$ and β are unknowns, these two constants can also be determined in terms of the least mean squares using the values of $n(\theta)$.

In the first step, multiple values of $L_{JA,\mathrm{directional}}$ for every azimuth angle, θ, were obtained. In order to obtain the value of a, average $L_{JA,\mathrm{directional}}$ ($\bar{L}_{JA,\mathrm{directional}}$) was used. The value of a is calculated as

$$a = \frac{10^{L_{JA,O}/10}}{10^{L_{JA,O}/10} + \int_0^{\pi/2}\int_0^{2\pi} 10^{\bar{L}_{JA,\mathrm{directional}}/10} \cos^{n_{\max}\sin^{\beta}\theta}\varphi \sin\varphi d\theta d\varphi}. \quad (27)$$

3.3.2. Results

The determined values of model parameters a, $n_{\max}$ and β are shown in Figs. 16(a), 16(b) and 16(c), respectively. In the figures, values of the parameters are arranged in a relationship with the open ratio, W/R. Regarding the variation of the values of the parameters owing to the differences of the dimensions of semi-underground roads, the following tendencies are seen.

[1] The values of a are in the range between 0.1 and 0.2 for all cases.

[2] The values of $n_{\max}$ are in the range between 1 and 2, and it becomes smaller with larger open ratio.

[3] A rough tendency that the values of β become larger with the open ratio can be seen, and β values scatter in the range between 1.6 and 2.7.

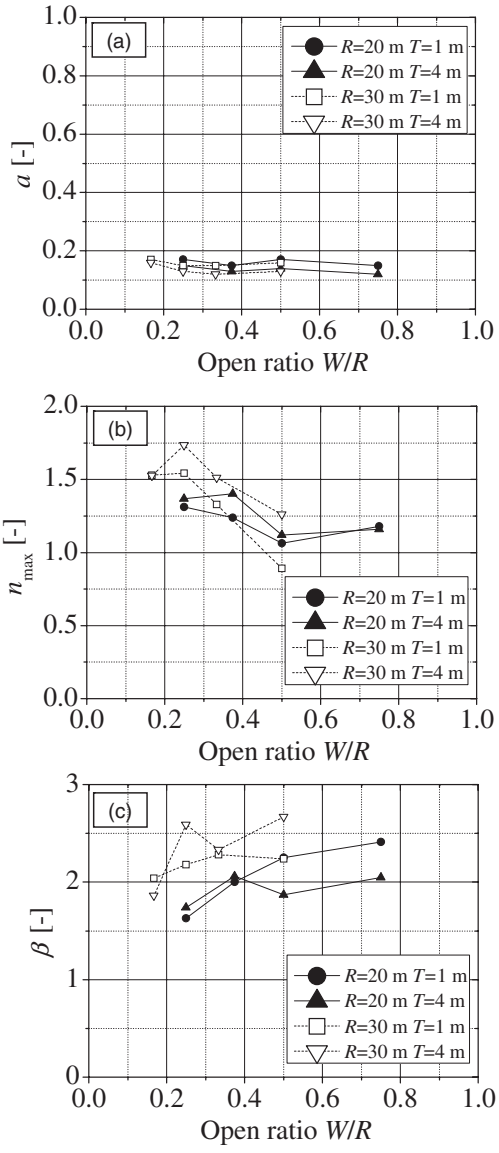

Fig. 16 Determined model parameters a, $n_{\max}$ and β.

4. INVESTIGATION OF SINGLE EVENT SOUND EXPOSURE LEVELS IN ROADSIDE AREA

In order to confirm the validity of the energy-based practical calculation model, the hypothetical point source method, A-weighted single event sound exposure levels in the roadside area were calculated by the hypothetical point source method and the results were compared with the calculation results obtained by FDTD analysis. Figure 17 shows sound sources and receiving points. Receiving points were distributed on a straight line, parallel to the road and 15 m from the center of the mouth. In the calculations using Eqs. (8), (9) and (10), the values of α, $n_{\max}$, β and the correction of $\Delta L_{\mathrm{dir,su}}$ were determined by the procedure described in 3.3.1. The values are shown in Table 2. The calculation results obtained using the practical calculation model and those obtained by FDTD

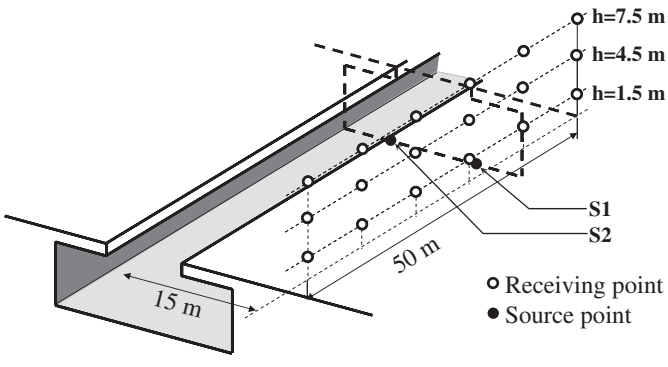

Fig. 17 Sources and receiving points for investigation of single event sound exposure levels in roadside area.

Table 2 Values of the parameters.

	a	β	$n_{\max}$	$\Delta L_{\mathrm{dir,su}}$ (dB)
Case 1	0.17	1.63	1.31	1.52
Case 2	0.15	2.00	1.24	1.39
Case 3	0.17	2.25	1.06	1.16
Case 4	0.15	2.41	1.18	1.24
Case 5	0.15	1.74	1.37	1.57
Case 6	0.13	2.06	1.40	1.54
Case 7	0.14	1.87	1.12	1.35
Case 8	0.12	2.05	1.16	1.37
Case 9	0.17	2.04	1.53	1.54
Case 10	0.15	2.18	1.54	1.55
Case 11	0.15	2.28	1.33	1.38
Case 12	0.16	2.24	0.89	1.03
Case 13	0.16	1.86	1.53	1.62
Case 14	0.13	2.59	1.74	1.59
Case 15	0.12	2.33	1.51	1.55
Case 16	0.13	2.67	1.26	1.28

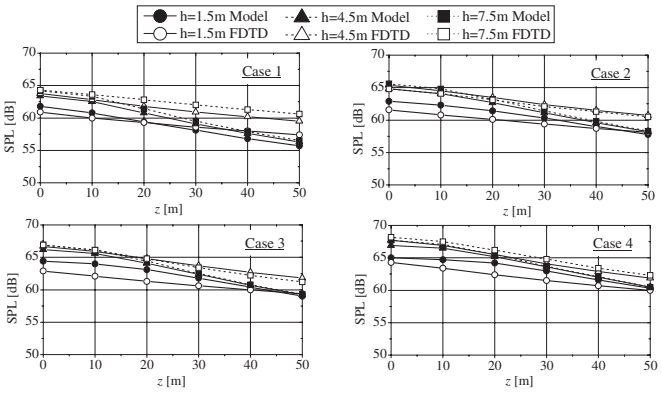

Fig. 18 Single event sound exposure levels in roadside area for Cases 1, 2, 3 and 4.

analysis for Case 1, Case 2, Case 3 and Case 4 are shown in Fig. 18. The correspondence between the model and the FDTD is fairly good. However, at receiving points far from the source, results of calculation using the model are lower than those of the FDTD analysis. This tendency is caused by a difference in the sound radiation characteristics in the longitudinal (small θ) direction. For the y-z plane ($\theta = 0$), as seen in Figs. 12(a) and 12(b), the directivity of sound radiation is modeled in the omnidirection by the practical calculation model, whereas the wave-based numerical analysis gave higher levels of sound radiation near $\varphi = 90^\circ$ in the longitudinal direction. The correspondence between the model and the FDTD analysis for all cases is shown in Fig. 19. The average difference for all points and the standard deviation of the differences were 0.05 dB and 1.45 dB, respectively.

5. CONCLUSIONS

An energy-based practical calculation method of road traffic noise in a roadside area of a semi-underground road

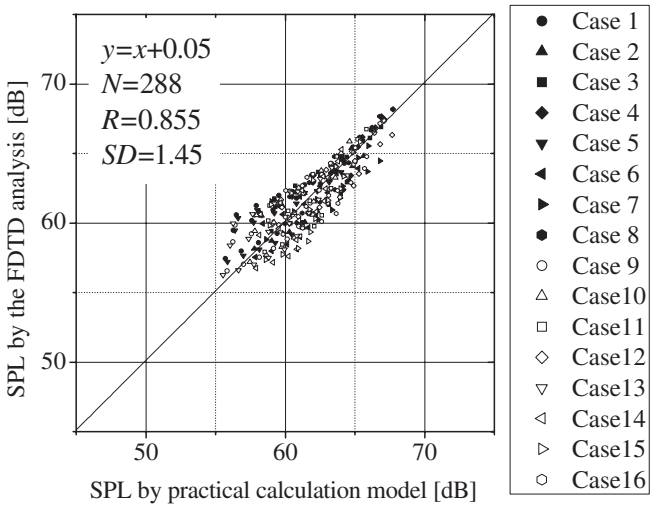

Fig. 19 Correspondence between the practical calculation model and the FDTD analysis.

was investigated by a wave-based numerical analysis with the finite-difference time-domain method. The practical calculation method, in which the sound source is simply modeled as a hypothetical point source with a specific directivity to the dimensions of the semi-underground road structure, has been proposed in ASJ RTN-Model 2003. In this study, values of parameters characterizing the directional characteristics of the hypothetical point source were determined for several cases, and a correction term regarding the sound energy of the hypothetical sound source was examined, on the basis of wave-based numerical analysis. For wave-based numerical analysis of sound propagation in a three-dimensional sound field around a straight semi-underground road, a technique of transformation from 2-D to 3-D using a Fourier-type integration was applied to transient responses obtained by two-dimensional finite-difference time-domain analysis. In this study, semi-underground roads with reflective boundaries were dealt with and noise reduction effects of absorptive treatment were not examined. To extend the applicability of this practical calculation method, it is necessary to further investigate road structures with finite impedance boundary conditions.

REFERENCES

[1] Research Committee of Road Traffic Noise in the Acoustical Society of Japan, "Road traffic noise prediction model "ASJ RTN-Model 2003" proposed by the Acoustical Society of Japan," *J. Acoust. Soc. Jpn.* (*J*), **60**, 215–217 (2004) (in Japanese).

[2] S. Sakamoto and H. Tachibana, "Experimental study on calculation model of road traffic noise radiated from semi-underground roads," *Proc. ICA 2004*, Vol. IV, pp. 3011–3014 (2004).

[3] S. Sakamoto, "Calculation of sound propagation in three-dimensional field with constant cross section by Duhamel's efficient method using transient solutions obtained by finite-

different time-domain method," *Acoust. Sci. & Tech.*, **30**, 72–82 (2009).
[4] J.-P. Berenger, "A perfectly matched layer for the absorption of electromagnetic waves," *J. Comput. Phys.*, **114**, 185–200 (1994).
[5] Q. Qui and T. L. Geers, "Evaluation of the Perfectly Matched Layer for computational acoustics," *J. Comput. Phys.*, **139**, 166–183 (1998).
[6] S. Sakamoto, "Phase-error analysis of high-order finite difference time domain scheme and its influence on calculation results of impulse response in closed sound field," *Acoust. Sci. & Tech.*, **28**, 295–309 (2007).

Shinichi Sakamoto was borne on June 10, 1968 in Saitama, Japan. He received B.E., M.E. and Doctor of Engineering degrees from The University of Tokyo in 1991, 1993 and 1996, respectively. Associate Professor of the Applied Acoustic Engineering Laboratory, Institute of Industrial Science, The University of Tokyo. His current research interests are in areas of architectural acoustics and environmental noise control engineering. He received the Awaya Prize Young Researcher Award and the Sato Prize Paper Award in 2001 and 2009, respectively. A member of ASA, ASJ, INCE/J and AIJ.